Rigorous Analysis of a Superconducting Hot-Electron Bolometer Mixer: Theory and Comparison with Experiment

R.S. Nebosis, A.D. Semenov, Yu.P. Gousev, and K.F. Renk

Institute of Applied Physics, University of Regensburg,
93040 Regensburg, Germany

Abstract

We present theoretical analysis of the performance of a superconducting hot-electron bolometer mixer with electron cooling due to electron phonon interaction. The analysis is based on a complete set of thermal balance equations for phonons and electrons. A non-thermal action of a dc current has been considered phenomenologically using an analytical fit of isothermal current-voltage characteristics of the mixer. The operation point of the mixer has been determined as a result of the heating by both the power of a local oscillator and the power dissipated by the current. Electron temperature fluctuations, Nyquist noise, and shot noise have been supposed to only contribute to the mixer noise. The conversion gain and the noise temperature of the mixer have been evaluated taking into account an electro-thermal feedback between the mixer and an intermediate frequency circuit with an arbitrary impedance. We have obtained general expressions for the conversion gain, noise temperature and impedance which enabled us to estimate ultimate performance of a superconducting hot-electron bolometer mixer. Theoretical predictions are in good agreement with experimental results obtained for a NbN hot-electron bolometer mixer at a radiation frequency of 2.5 THz.

I. Introduction

Recently there has been increasing interest in superconducting hot electron bolometer (HEB) mixers that are considered as promising candidates for heterodyne receivers in the THz frequency range [1]. Theoretical analysis of a superconducting film HEB mixer utilizing the electron-phonon cooling mechanism was presented for the first time by Gershenzon et. al. [2]. Karasik and Elant'ev (KE) [3] have generalized the theory taking into account a feedback between the mixer and an intermediate frequency circuit. Both considerations treated phonons in the film as a heat sink with ambient temperature. This is an adequate approach for conventional low temperature superconducting materials, e.g. Nb, where the ballistic propagation of thermal phonons in the films ensures a cooling rate of phonons much larger than that of electrons. Since HEB mixers based on different superconducting materials are presently under development there is a need to further generalize the theory for a case when the phonon cooling rate is comparable (NbN) or even smaller (YBCO) than the cooling rate of electrons.

In this paper we present a rigorous analysis of a superconducting HEB mixer with phonon cooling mechanism for arbitrary cooling rates and specific heats of electrons and phonons. The paper is organized as follows. In Section II we discuss a physical model and approximations used to derive heat balance equations and a phenomenological expression describing a non-thermal effect of the current. In Section III we obtain current-voltage characteristics of the mixer in the operation point that is determined by the ambient temperature and the power of a local oscillator. The performance of the mixer, i.e. conversion gain, noise temperature, and output impedance, are evaluated in Section IV. Experimental technique and samples are described in Section V. Results of the experimental study of a NbN HEB mixer in comparison with theoretical predictions are presented in Section VI. An estimate of the ultimate performance of a HEB mixer for different superconducting materials is given in Section VII.

II. Basic Considerations

A hot-electron bolometer mixer, usually a structured superconducting film on a dielectric substrate, can be thought of as a system consisting of the electron and phonon subsystem in the film, and the phonon subsystem in the substrate, each thermally coupled to the other. When the mixer is illuminated by radiation or biased with a dc voltage, the power of radiation (or electric power) is primarily absorbed by electrons in the film. The absorbed power is then transferred to phonons via electron-phonon interaction and, consequently, to the substrate by phonons leaving the film. It is experimentally verified that the temperature of the substrate can be considered as almost constant and equal to the ambient temperature (T_0). Neglecting diffusion processes in the plane of the film and assuming that different effective temperatures, Θ and T_p, can be assigned to electrons and phonons in the film, the energy flow through the whole system is described by a set of coupled heat balance equations [4]

$$c_e(\Theta)V\frac{\partial\Theta}{\partial t} = -w_1(\Theta;\ T_p) + UI + \alpha[\sqrt{P_S}\exp(j\Omega_1 t) + \sqrt{P_{LO}}\exp(j\Omega_2 t)]^2 \tag{1a}$$

$$c_p(T_p)V\frac{\partial T_p}{\partial t} = -w_2(T_p;\ T_0) + w_1(\Theta;\ T_p), \tag{1b}$$

where c_e, c_p are specific heats of electrons and phonons in the film, V is the volume of the mixer, UI is the dissipated electrical power (I and U are dc current and voltage), Ω_1 and Ω_2 are radiation frequencies of the signal and the local oscillator, respectively. In terahertz heterodyne receivers the signal radiation and the radiation of the local oscillator are usually delivered to the mixer by the same quasi optical antenna system. Assuming that the local oscillator is appropriately matched to the antenna we suggest, hereafter, the same optical loss $L_{OPT} = -10\ lg(\alpha)$ for signal radiation and for the radiation of the local oscillator. Thus, radiation powers of the signal (P_S) and of the local oscillator (P_{LO}) are both referred to the receiver input. For a relatively thin film thermally well coupled to a substrate, heat diffusion in the direction normal to the film plane can be neglected. Terms in (1a/b) describing the heat out-flow from electrons to phonons and from phonons to the substrate are then given [4] by $w_1 = V A_e(\Theta^n - T_p{}^n)$ and $w_2 = V A_p(T_p^4 - T_0^4)$, respectively, where A_e, A_p and n are material constants. The factor n depends on the superconducting material as follows, $n = 4$, 3.6, and 3 for Nb, NbN, and YBaCuO respectively. Using specific heats of electrons and phonons, the electron-phonon interaction time τ_{e-p}, and the characteristic time of phonon escape from the film τ_{es}, constants A_e and A_p can be written [2,3] as $A_e = c_e/(n\Theta^{n-1}\tau_{e-p})$ and $A_p = c_p/(4T_p^3\tau_{es})$. For $|\Theta - T_0| \ll T_0$ heat out-flow terms can be linearized to $w_1 = V c_e(\Theta - T_p)/\tau_{e-p}$ and $w_2 = V c_p(T_p - T_0)/\tau_{es}$.

In order to obtain a general solution of heat balance equations one has to make a certain assumption on how the dc resistance of the mixer R depends on the current and the electron temperature. The dependence of the resistance on the electron temperature $R(\Theta)$ can be taken from the experiment or modelled analytically. With respect to the current the simplest approximation is to neglect the non-thermal dependence $R(I)$ and only consider the effect of the current via a change of the electron temperature due to Ohmic heating. This approximation fails at small currents where Ohmic heating plays a minor role and $R(I)$ dependence is determined mostly by a particular mechanism of resistivity (e.g. phase slip centers or vortex flow). Though, for a particular case, the exact form of $R(I)$ can be only found experimentally, different mechanisms of resistivity lead to apparently close results [5,6]. Basing on isothermal voltage-current characteristics reported by Elant'ev et al. [6] for Nb superconducting films, we model the film resistance as

$$R(I;\Theta) \approx \frac{R_n(\Theta)}{2}\left(1 + f(\Theta) - \frac{[1-f(\Theta)]^3}{[1+I/I_0 - f(\Theta)]^2}\right) \tag{2}$$

$$f(\Theta) = \frac{1}{1 + exp(4\frac{T_c-\Theta}{\Delta T_c})}$$

where T_c is the superconducting transition temperature of the film, ΔT_c is the transition width (10 % to 90 % of the normal state resistance), and $R_n(\Theta)$ is the temperature dependent normal state resistance. The fitting parameter I_0 corresponds to the current at which isothermal voltage-current $U(\Theta = const, I)$ characteristics become linear, i.e. $dU(\Theta = const, I)/dI \approx const$ for $I \gg I_0$. For small currents ($I \approx 0$), when the electron temperature Θ is nearly equal to the ambient temperature T_0, Eq. 2 becomes $R(T_0) = R_n(T_0)f(T_0)$ that describes well a typical superconducting transition.

III. Voltage-Current Characteristics of the HEB

A HEB mixer is usually operated at an ambient temperature below the transition temperature. When a local oscillator is applied the absorbed radiation power drives the mixer into the operation point whereby the electron temperature is close to T_c and the mixer dc resistance is non-zero. Assuming that the influence of the local oscillator is essentially thermal we obtain the electron temperature in the operation point as a solution of non-linearized heat balance equations for steady state conditions

$$0 = -A_e V(\Theta^n - T_p^n) + \alpha P_{LO} + I^2 R(I;\Theta) \tag{3a}$$

$$0 = A_e V(\Theta^n - T_p^n) - A_p V \tau_{es}(T_p - T_0). \tag{3b}$$

At the first stage, setting $I = 0$, we evaluate the effective temperatures Θ_l and T_{pl} due to the heating by the local oscillator alone. In a real experiment the mixer is operated within the superconducting transition. Thus, the further rise of effective temperatures due to Ohmic heating by the current is always less than ΔT_c that, in turn, is usually much less than T_c. Therefore, we assume for the effective temperatures, with a current applied, $\Theta = \Theta_l + \delta\Theta$ and $T_p = T_{pl} + \delta T_p$ where $\delta\Theta \ll \Theta$ and $\delta T_p \ll T_p$. We further suggest $R(I,\Theta) = R(I,\Theta_l) + \delta\Theta(\partial R/\partial\Theta)$ and solve equations (3a/b), now in the linearized form, for δT_p and $\delta\Theta$. The result is

$$\delta\Theta(I) = \frac{I^2 R(I;\Theta_l)}{\kappa - I^2 \partial R/\partial\Theta} \quad \text{with} \quad \kappa = V A_e n \Theta_l^{n-1}\left(1 + \frac{nA_e}{4A_p} T_{pl}^{n-4}\right)^{-1}. \tag{4}$$

Combining (2) and (4) we obtain voltage-current characteristics of the mixer for different ambient temperatures and LO powers

$$U(I) = IR(I, \Theta_l + \delta\Theta(I)). \tag{5}$$

Fig. 1 shows a set of $I - U$ curves calculated for different ambient temperatures. For calculations we used typical parameters of a NbN mixer which are listed in Table I.

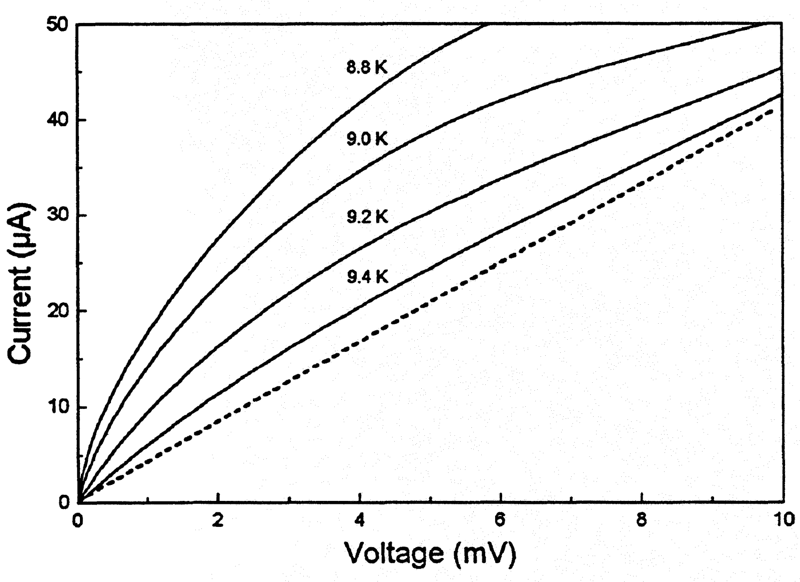

Fig. 1. Calculated current-voltage characteristics of a typical NbN HEB for different ambient temperatures. The dashed line corresponds to the normal state.

Table I. Parameters used for model simulations; l, b, and d are the length, width, and thickness of the mixer.

$R_n(T_c)$	T_c	ΔT_c	l	b	d	c_e	c_p	τ_{es}	τ_{e-p}	αP_{LO}	I_0
Ω	K	K	μm	μm	nm	mJ/(cm^{3}K)	mJ/(cm^{3}K)	ps	ps	μW	μA
245	11.3	0.4	2	2	6	1.5	10.5	50	10	3.5	70

Values of c_p, c_e, τ_{e-p}, and τ_{es} correspond to the transition temperature. For small voltages the curves can be approximated by $I(U) \approx U/[R_n(T_0)f(T_0)]$ where T_0 is the ambient temperature. For larger voltages, as long as Ohmic heating is relatively small, the shape of $I-U$ curves is almost determined by the non-thermal, current induced change of the resistance. With a further increase of the voltage Ohmic heating becomes considerable ($\delta\Theta \sim \Delta T_c$). In this region the shape of the curves is determined by the dependence of the mixer resistance on the electron temperature $I \approx U/R(\Theta)$. Equations (4) and (5) are only applicable, as long as either the ambient temperature is close to T_c or the local oscillator drives the electron temperature to a value close to T_c, so that $R(I \approx 0)$ is non-zero.

IV. Impedance, Conversion Gain, Noise Temperature

The impedance of the mixer is formally given by the expression

$$Z = \frac{\mathrm{d}U}{\mathrm{d}I} = \frac{\mathrm{d}}{\mathrm{d}I}[IR(I,\Theta)] = R(I,\Theta) + I\frac{\partial R}{\partial I} + I\frac{\partial R}{\partial \Theta}\frac{\mathrm{d}\Theta}{\mathrm{d}I}. \tag{6}$$

The term $\partial R/\partial I$ corresponds to a non-thermal action of the current. As relevant mechanisms usually have characteristic times small compared to the reciprocal bandwidth of the mixer we hereafter neglect the frequency dependence of this term. The quantity $\mathrm{d}\Theta/\mathrm{d}I$ is evaluated assuming that a small change of the current $\mathrm{d}I = \delta I exp(j\omega t)$ causes a change of the electron temperature $\mathrm{d}\Theta = \delta\Theta exp[j(\omega t + \varphi_1)]$ and, consequently, a change of the phonon temperature $dT_p = \delta T_p exp[j(\omega t + \varphi_2)]$. Substituting dI, $d\Theta$, and dT_p in linearized heat balance equations and solving it together with (6) we find

$$Z(\omega) = \frac{\psi(\omega)Z(\infty) + CR}{\psi(\omega) - C} \tag{7}$$

$$\text{with } \psi(\omega) = \frac{(1 + j\omega\tau_1)(1 + j\omega\tau_2)}{(1 + j\omega\tilde{\tau})} \; ; \; Z(\infty) = R + I\frac{\partial R}{\partial I} \; ; \; C = I^2\frac{\partial R/\partial\Theta}{c_e V}\tau_\Theta$$

$$\text{and } \tau_\Theta = \tau_{e-p} + \frac{c_e}{c_p}\tau_{es} \; ; \; \tilde{\tau} = \frac{1}{\Gamma_p + \Gamma_s}$$

$$\tau_{1,2}^{-1} = \frac{\Gamma_e + \Gamma_p + \Gamma_s}{2}\left(1 \pm \sqrt{1 - \frac{4\Gamma_e\Gamma_s}{(\Gamma_e + \Gamma_p + \Gamma_s)^2}}\right)$$

$$\Gamma_e = \frac{1}{\tau_{e-p}} \; ; \; \Gamma_p = \frac{c_e}{c_p}\Gamma_e \; ; \; \Gamma_s = \frac{1}{\tau_{es}}.$$

In the limiting case $c_p\tau_{e-p}/c_e \gg \tau_{es}$ this expression can be reduced to

$$Z(\omega) = \frac{(1 + j\omega\tau_\Theta)Z(\infty) + CR}{(1 + j\omega\tau_\Theta) - C}$$

that coincides with the formula for a Nb HEB found in [3] or, more generally, for any bolometer where the heat out-flow can be described with only one time constant (lumped bolometer) [7]. The self heating parameter C describes the thermal run-out of a mixer operated in the current mode. The impedance of the mixer is purely real for $\omega = 0$ and for $\omega \to \infty$. The physical reason is that for low frequencies the electron temperature instantaneously follows oscillations of the absorbed electrical power. For extremely high frequencies the temperature cannot follow oscillations of the power and the impedance is determined by the non-thermal action of the current. In both cases there is no phase shift between current and voltage oscillations.

To derive an expression for the conversion efficiency of the mixer we first obtain the responsivity of the device in a video detection regime. Since we are interested in the voltage registered by the readout electronics, we introduce an equivalent impedance Z_L of a circuit (load) connected to the mixer output and calculate the voltage drop dU_L across the load. An electro-thermal feedback between the mixer and the load is taken into account assuming that

$$dU_L = -\,dU = dI\ Z_L \tag{8}$$

where dI is the signal current through the load (equal to the signal current through the mixer) and dU is the voltage over the mixer. The connection between a small variation (dP) of the power of incoming radiation and the corresponding variation of the voltage is formally given by

$$\frac{dU}{dP} = \frac{d}{dP}[IR(I,\Theta)] = R\frac{dI}{dP} + I\frac{\partial R}{\partial I}\frac{dI}{dP} + I\frac{\partial R}{\partial\Theta}. \tag{9}$$

To evaluate $d\Theta/\,dP$ we use the same procedure as has been used for the evaluation of the mixer impedance. Substituting $dP = \delta P exp(j\omega t)$ and corresponding variations of Θ, T_p, and I in linearized heat balance equations we obtain, using (8) and (9), the frequency dependent responsivity

$$S(\omega) = \frac{\mathrm{d}U_L}{\mathrm{d}P} = \frac{\alpha}{I} \frac{CZ_L}{C(R - Z_L) + (Z(\infty) + Z_L)\psi(\omega)}. \tag{10}$$

For $c_p\tau_{e-p}/c_e \gg \tau_{es}$ this expression coincides with that derived for a lumped bolometer [3]. We shall point out that general expressions for the mixer impedance and responsivity can be obtain via a formal replacement of the frequency dependent term $1 + j\omega\tau_\Theta$ in formulas for a lumped bolometer by the more general term $\psi(\omega)$. To evaluate the conversion gain and the noise temperature of the mixer we use general expressions for the impedance (7) and the responsivity (10) and follow the approach suggested by KE [3]. The shot noise is included into consideration assuming that it can be presented as an equivalent noise source $\sqrt{(l_i/l)}Z(\infty)\sqrt{Ie}$ that acts similar to the source representing Nyquist noise $\sqrt{4k_B\Theta Z(\infty)}$. The pre factor l_i/l, where l_i is the elastic mean free path of electrons and l is the mixer length along the current path, determines the part of electrons passing the sample ballistically and, thus, contributing to the shot noise. The conversion gain is given by

$$\eta(\omega) = \frac{2|S(\omega)|^2}{Z_L} P_{LO} = \frac{2\alpha^2}{I^2} \frac{R_L}{R_L + Z(\infty)} \frac{C^2 P_{LO}}{[C\frac{R - R_L}{R_L + Z(\infty)} + \xi]^2 + \varphi^2} \tag{11}$$

with

$$Z(\infty) = R(\Theta; I) + \frac{IR_n(\Theta)}{I_0} \frac{[1 - f(\Theta)]^3}{[1 + I/I_0 - f(\Theta)]^2};$$

$$C(I; \Theta) = I^2 \frac{\tau_\Theta}{c_e V} \frac{R_0 f(\Theta)}{\Theta_c} \left[1 + \frac{4\Theta}{\Delta\Theta_c} f(\Theta)\ exp\left(4\frac{\Theta_c - \Theta}{\Delta\Theta_c}\right)\right];$$

$$\xi(\omega) = \frac{1 + \omega^2(\tau_1\tilde{\tau} + \tau_2\tilde{\tau} - \tau_1\tau_2)}{1 + (\omega\tilde{\tau})^2}; \quad \varphi(\omega) = \frac{\omega(\tau_1 + \tau_2 - \tilde{\tau}) + \omega^3\tau_1\tau_2\tilde{\tau}}{1 + (\omega\tilde{\tau})^2}$$

where P_{LO} is the power of the local oscillator at the system input and $\psi(\omega) = \xi(\omega) + j\varphi(\omega)$ (see Eq. 7). The system single side band noise temperature is

$$T_{SSB} = \left[\frac{2\Theta RI^2}{\alpha^2 C^2 P_{LO}} + \frac{l_i}{l} \frac{eI^3R^2}{\alpha^2 k_B C^2 P_{LO}}\right] \cdot (\xi^2 + \varphi^2) + \frac{2\Theta^2 G_0}{\alpha^2 P_{LO}} + \eta(\omega)^{-1} T_A \tag{12}$$

where T_A is the noise temperature of an amplifier connected to the mixer. The terms in square brackets represent contributions of the Nyquist noise and shot noise respectively, the second term represents the contribution due to thermal fluctuations of the electron temperature, and the fourth term is the contribution of the amplifier. Results of calculations with parameters listed in Table 1 are shown in Fig. 2. Additionally we assumed $\alpha = 0.027$, $P_{LO} = 126\mu W$, and $I = 40\ \mu A$. The conversion gain is constant for low frequencies and decreases at frequencies higher than the roll-off frequency. If the matching between the mixer and the load is not perfect ($Z_L > R$) the self heating causes a shift of the roll-off frequency to a lower value. The single side band noise temperature due to thermal fluctuations only is frequency independent because the noise voltage produced by this fluctuations has the same frequency dependence as the conversion gain.

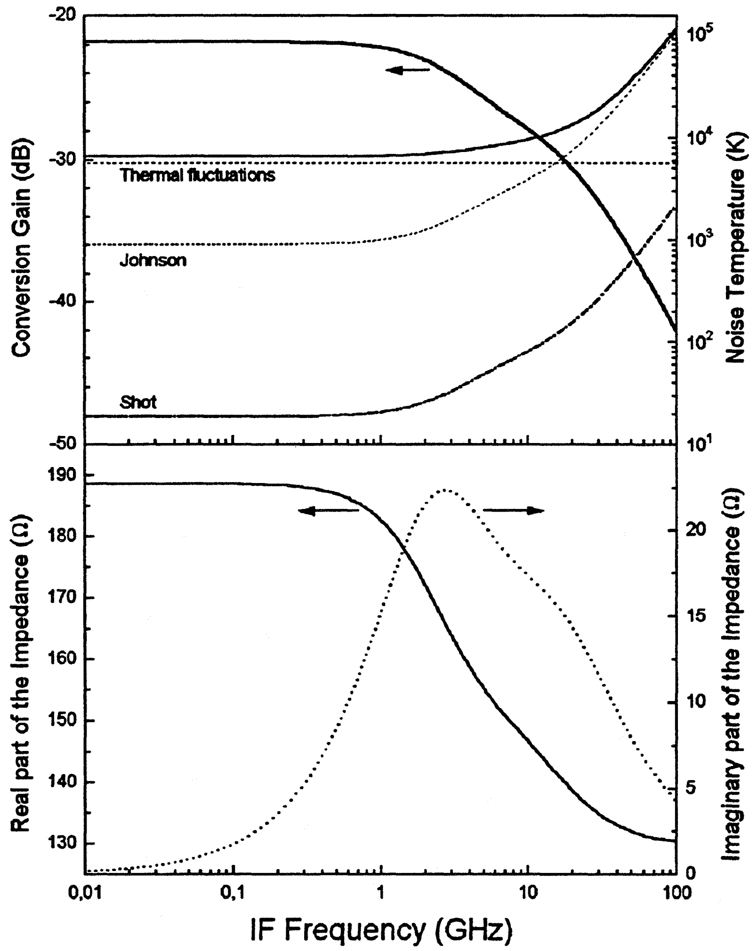

Fig. 2. Conversion gain (upper panel), single side band noise temperature (upper panel), and impedance (real and imaginary parts, lower panel) as functions of the intermediate frequency. Contributions to the noise temperature (solid line) due to the Nyquist noise (dashed line), shot noise (dashed-dotted line), and thermal fluctuations (dotted line) are shown separately.

The Nyquist noise and the shot noise produce contributions to the noise temperature which increase with frequency because the Nyquist noise and the shot noise are frequency independent. The contribution of the shot noise to the noise temperature is almost negligible since $l_i/l \approx 10^{-3}$ ($l_i \approx 1$ nm for NbN [8]). Here one interesting aspect has to be emphasized. Due to the self heating the bandwidth determined via the noise temperature differs from that determined via the conversion gain. An increase of the noise temperature occurs at a frequency higher than the roll-off frequency of the conversion gain (Fig. 2). The imaginary part of the mixer impedance becomes considerable only for frequencies between 1 and 20 GHz and for rather large self heating parameters ($C > 0.1$). The real part of the impedance has the value $[CR + Z(\infty)]/(1 - C)$ at the low-frequency plateau and decreases to $Z(\infty)$ at higher frequencies. This behaviour corresponds to experimental observations [6].

V. Samples and Experimental Technique

We studied a hot-electron bolometer made from a 6 nm thick NbN film that was grown on the sapphire side of a 0.35 mm thick silicon-on-sapphire wafer by dc magnetron sputtering of a Nb target in Ar+N_2

atmosphere. The film was patterned (Fig. 3a) to form three parallel bridges, each 0.7 μm wide and 2.0 μm long, spaced by 1.2 μm wide blanks.

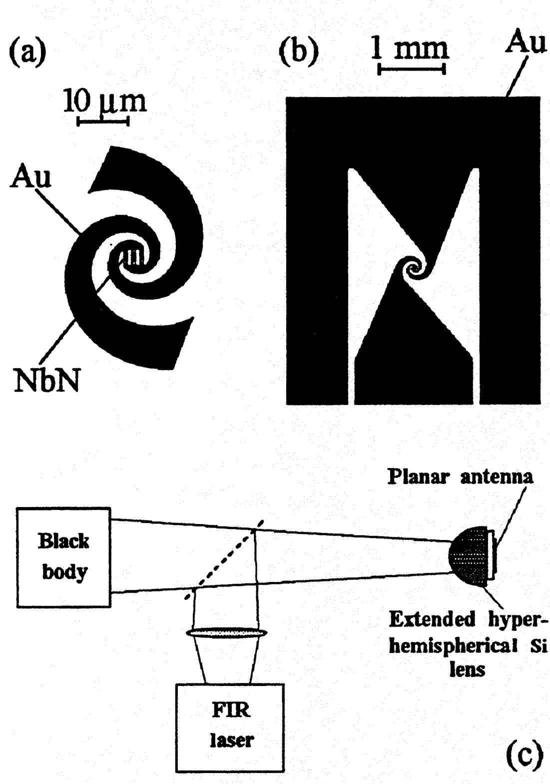

Fig. 3. The inner part of the planar antenna with the NbN hot-electron bolometer (a), the planar antenna integrated into the co-planar transmission line (b), and optical scheme of the experiment (c).

The structure was connected to the terminals of a planar self-complementary logarithmic spiral antenna integrated into a co-planar transmission line (Fig. 3b). The antenna and the co-planar line were structured from a 150 nm thick gold film thermally evaporated on the same wafer over a 20 nm thick Ti buffer layer. A 6×6 mm^2 mixer chip was cut out of the wafer and clamped mechanically with the silicon side to an extended hyperhemispherical silicon lens (Fig. 3c). The sample had a superconducting transition temperature T_c = 11.3 K and a transition width of $\approx$ 0.4 K. We used a silicon lens with a radius of 6.3 mm and an extension length of 2.35 mm whereby the antenna was positioned at the second focus of the corresponding synthesized elliptical lens [9]. The radiation pattern of this hybrid antenna (the planar antenna with the lens) was rotationally symmetric with a full width of the main lobe of $\approx$ 1 degree (- 3 dB level) and with first side lobes below a level of - 8 dB. The corresponding effective area of the hybrid antenna was almost half of the cross-section area of the silicon lens. The mixer with the hybrid antenna was mounted in a vacuum chamber on the cold finger of a temperature variable cryostat with optical access through a mylar window. The ambient temperature of the mixer was measured at the cold finger of the cryostat. As a local oscillator we used a cw gas laser delivering radiation in a fundamental Gaussian mode at a frequency of 2.52 THz. The laser beam was focused by a TPX plano-convex lens to match the radiation pattern of the hybrid antenna. The radiation of the local oscillator and radiation of a black body thermal source were diplexed with a grid polarizer in front of the cryostat window. The power of the radiation of the local oscillator (LO power) was measured in the plane of the cryostat window with a calibrated Golay cell detector. Thermal radiation was modulated with a chopper. The output signal of the mixer at the intermediate frequency was guided out of the cryostat by a flexible co-planar line, amplified by room temperature amplifiers (noise temperature 60 K, bandwidth 0.7 GHz centered at 1.5 GHz), rectified by a calibrated square-law semiconductor detector, and registered at the chopping frequency by a lock-in amplifier; thus we monitored black body radiation within both side bands. The chopper was covered with an absorber and, therefore, represented a black body radiation source at room temperature. The temperature of the hot thermal source was 900 K. A filter placed between the hot source and the polarizer blocked broad band near-infrared radiation. Instead of the hot thermal source, we alternatively used a cold source with a temperature of 77 K.

VI. Experimental Results in Comparison with Calculations

Voltage-current characteristics of the mixer measured at an ambient temperature of 8.8 K for different powers of the local oscillator are shown in Fig. 3. We fitted experimental curves varying α and I_0 (see Sec. III). We used an iteration which consisted of two repetitive steps. First, varying α, we adjusted the slope of the calculated curves to that of experimental ones at small voltages (< 0.5 mV). Second, we varied I_0 to adjust the slope at larger voltages (> 4 mV). The best coincidence was achieved for $I_0 = 70\ \mu$A and $\alpha = 0.027$ that corresponded to an optical loss (L_{OPT}) of - 15.6 dB.

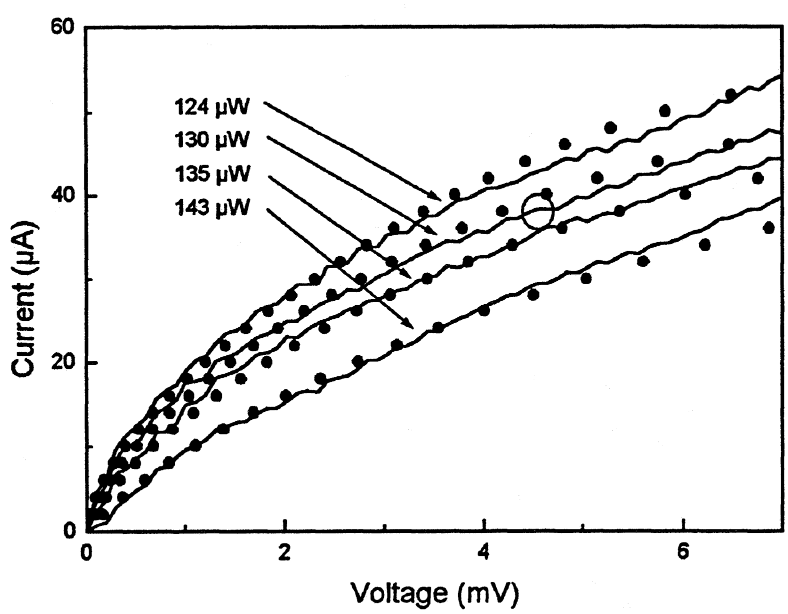

Fig. 4. Current-voltage characteristics of the mixer for different powers of the local oscillator. Closed circles represent the best model fit with $I_0 = 70\ \mu$A and $\alpha = 0.027$. Open circle indicates the operation point.

At the operation point ($I = 38\ \mu$A, $P_{LO} = 130\ \mu$W, $T_0 = 8.8$ K) we measured [10] a Y-factor of 1.018 indicating a double side band system noise temperature $T_{DSB} \approx 40000$ K; with the cold load (having a slightly larger aperture) we obtained a slightly smaller noise temperature ($\approx$ 32000 K). Assuming an appropriate matching of the thermal sources to our mixer we estimated from the measured IF signal a total conversion loss (L) of 25 dB. With the amplifier noise temperature $T_A = 60$ K we concluded a mixer noise temperature $T_M = T_S - 10^{0.1L}\ T_A \approx 20000$ K and a sum of the conversion loss (L_M) of the mixer and the loss (L_{IF}) due to impedance mismatch at the intermediate frequency $L_M + L_{IF} = L - L_{OPT} \approx 9$ dB. We suggest that, because of a relatively high differential resistance of the mixer in the operation point, these losses are mostly due to the impedance mismatch between the mixer and the intermediate frequency circuit. For our experimental conditions with best fit values of I_0 and α we calculated, using equations (12) and (11), $T_{DSB} = T_{SSB}/2 = 6500$ K and $\eta = 8.810^{-3}$ that corresponded to $L = 20.5$ dB. This value is 4.5 dB smaller than the conversion loss (25 dB) obtained experimentally. We believe that the discrepancy occurred mostly because of a non-perfect matching of the thermal radiation source to the mixer and losses in the diplexer. The former resulted in a worse optical coupling of the signal radiation compared to that of the local oscillator. Correcting the calculated value for the discrepancy we estimated a DSB system noise temperature of $\approx$ 19000 K.

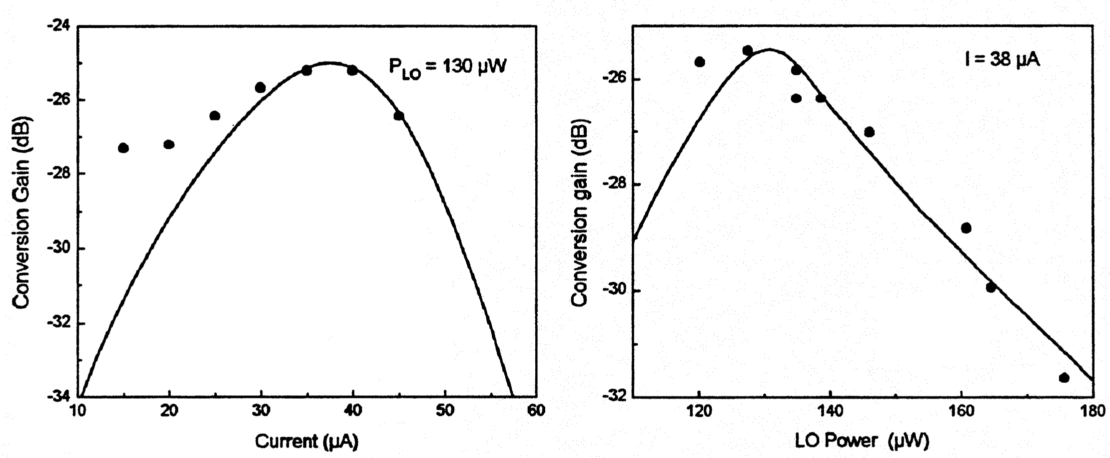

Fig. 5. Conversion gain of the nixer (•) for different currents (left panel) and LO powers (right panel). Calculated conversion gain (solid lines) is decreased by 4.5 dB.

The output signal of the mixer is shown in Fig. 5 for different currents (left panel) and powers (right panel) of the local oscillator. In both cases there is a maximum of the signal which occurs at the electron temperature $\Theta \approx T_c$ where the steepness of the superconducting transition reaches the largest value. The maxima of the signal are slightly asymmetric due to a direct, non-thermal contribution of the current to the conversion gain of the mixer. Model simulations corrected for the discrepancy (4.5 dB) are in good coincidence with experimental data. A deviation of experimental points from the calculated dependences occurring at small currents and LO powers is due to a change of the mixer impedance caused by non sufficiently suppressed broad band near-infrared radiation of the hot thermal source. The reason for such an effect can be clearly seen in Fig. 4. At currents less than 20 μA the differential resistance decreases with a decrease of the LO power while at larger currents (> 30 μA) it remains constant. The further improvement of the optical coupling may be achieved making use of an antireflex coating for the silicon lens, a low noise amplifier, and better filtering of the broadband radiation.

VII. Ultimate Performance of HEB Mixers

We now estimate an ultimate performance of mixers from two materials (NbN and $YBa_2Cu_3O_{7-\delta}$) presently used for fabrication of HEB devices. We use Eqs. 11, 12 with an understanding that a real HEB of a submicron size should reveal, in addition to the phonon cooling mechanism, a contribution of the out-diffusion cooling [11]. Currently available NbN technology allows to fabricate a mixing element with a lateral size of 0.7 $\mu m \times 0.7\ \mu m$ and a thickness of 3 nm. We assume that the mixer has a transition temperature of 10 K and a transition width of 0.2 K. The operation current and the fitting parameter (I_0) are scaled in proportion to the cross section of the mixer, thus resulting in $I = 6\ \mu$A and $I_0 = 10\ \mu$A. For an ambient temperature of 4.2 K, assuming $\alpha = 1$ and $T_A = 0$, we find an optimal power of the local oscillator of $\approx 0.5\ \mu$W, a conversion gain of +0.1 dB, and a SSB noise temperature of $\approx$ 90 K for an IF frequency of 1.5 GHz. Corresponding intermediate frequency band is 8 GHz. With the use of the antenna system described in this paper and a commercially available low noise amplifier (T_A = 20 K) one could expect a system DSB noise temperature of $\approx$ 1500 K that corresponds to ten times quantum limit at a frequency of 2.5 THz.

Mixers based on high-temperature superconducting films are of interest for space THz applications as they are expected [3] to require a relatively small LO power and to be operated at liquid nitrogen temperatures. To date no noise temperature measurements have been reported for HTSC mixers, therefore the applicability of our model to HTSC materials is under debate. Additional noise mechanisms [12] and N-S domain structure of the resistive state [13], not included in our model, may strongly influence the bandwidth and the noise temperature of the mixer. Thus the estimation below can be thought of as a guideline for future studies. We consider an $YBa_2Cu_3O_{7-\delta}$ mixer with a lateral size 1 $\mu m \times 1\ \mu m$ made from a 15 nm thick film. Using material parameters (c_e, c_p, τ_{e-p}, and τ_{es}) for the actual film thickness at $T_c \approx 90$ K [14], assuming an operation current of 250 μA [15], $I_0 = 600\ \mu$A, $R_n = 100\ \Omega$, and $\Delta T_c = 1$ K we found at an ambient temperature of 77 K an optimal absorbed LO power of $\approx 140\ \mu$W. Calculated conversion gain (Fig. 6) exhibits a low frequency plateau with a SSB noise temperature of $\approx$ 70 K ($\alpha = 1, T_A = 0$) and a high frequency plateau with $T_{SSB} \approx 12000$ K.

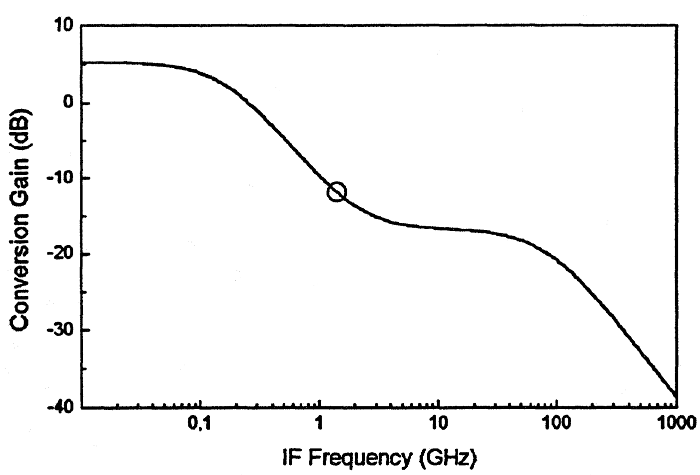

Fig. 6. Calculated conversion gain of an $YBa_2Cu_3O_{7-\delta}$ mixer. The open circle indicates the point corresponding to a SSB noise temperature of $\approx$ 3000 K.

Though the estimated noise temperature is less than that of best Shottky diodes [16] the LO power remains relatively large. A further decrease of the LO power is anambiguously connected with a decrease of the mixer volume; the noise temperature can be additionally lowered by decreasing the width of the superconducting transition.

Conclusion

We developed a rigorous phenomenological description of a novel superconducting hot-electron bolometer mixer with the phonon cooling mechanism. The model has been experimentally verified by analysing results of the experimental study of the NbN HEB mixer at 2.5 THz. We calculated a system noise temperature ($\approx$ 19000 K) close to the value observed in the experiment ($\approx$ 40000 K) and found a good agreement between theoretical simulations and experimental dependencies of the conversion gain on the LO power and current. We estimated an ultimate noise temperature of approximately ten times quantum limit at 2.5 THZ and an IF bandwidth of $\approx$ 8 GHz for currently available NbN devices. This performance promotes NbN HEB mixers to attractive candidates for aircraft based THz heterodyne receivers.

Acknowledgement

The work was supported by the Bundesministerium für Bildung, Wissenschaft, Forschung und Technologie (BMBF) - Förderkennzeichen 13N6413/0.

References

[1] Proc. of the 6th Int. Symp. on Space Terahertz Tech., 21-23 March, Caltech, Pasadena, USA (1995); Proc. of the Applied Superconductivity Conference, IEEE Trans. on Appl. Supercond. **5** (2) (1994); E. Gerecht, C.F. Musante, C.R. Lutz, Jr., Z. Wang, J. Bergendahl, K.S. Yngvesson, E.R. Mueller, J. Waldmann, G.N. Gol'tsman, B.M. Voronov, and E.M. Gershenzon, Proc. of the Int. Semicond. Device Res. Symp., UVa, USA, 619-622 (1995).

[2] E.M. Gershenzon, G.N. Gol'tsman, I.G. Gogidze, Yu.P. Gousev, A.I. Elant'ev, B.S. Karasik, and A.D. Semenov, Sov. J. Superconductivity **3**, 1582 (1990).

[3] B.S. Karasik, and A.I. Elant'tev, Proc. of the 6th Int. Symp. on Space Terahertz Tech., 21-23 March, Caltech, Pasadena, USA, 229 (1995).

[4] M.L. Kaganov, I.M. Lifshitz, and L.V. Tanatarov, Sov. Phys. JETP **4**, 173 (1957);
N. Perrin, and C. Vanneste, Phys. Rev. B **28**, 5150 (1983);
A. Frenkel, Phys. Rev. B **48**, 5150 (1993).

[5] T.T.M. Palstra, B. Batlog, R.B. van Dover, L.F. Schneemeyer, and J.V. Waszczak, Appl. Phys. Lett. **54**, 763 (1983);
Q.Y. Ying, and H.S. Kwok, Phys. Rev. B **42**, 2242 (1990);
A.M. Kadin, K. Epstein, and A.M. Goldman, Phys. Rev. B **27**, 669 (1983);
V.P. Galaiko, Sov. Phys. JETP **41**, 108 (1975);
W.J. Skocpol, M.R. Beasley, and M. Tinkham, J. Low Temp. Phys. **16**, 145 (1974).

[6] A.I. Elant'ev, and B.S. Karasik, Sov. J. Low Temp. Phys. **15**, 379 (1989).

[7] J.C. Mather, Appl. Opt. **21**, 1125 (1982).

[8] Yu.P. Gousev, A.D. Semenov, G.N. Gol'tsman, A.V. Sergeev, and E.M. Gershenzon, Physica B **194-196**, 1355 (1994).

[9] D.F. Fillipovic, S.S. Gearhart, and G.M. Rebeiz, IEEE Trans. on Microwave Theory and Tech. **41**, 1738 (1993).

[10] A.D. Semenov, Yu.P. Gousev, R.S. Nebosis, K.F. Renk, P. Yagoubov, B.M. Voronov, V.D. Syomash, and E.M. Gershenzon, submitted to Appl. Phys. Lett.

[11] D.E. Prober, Appl. Phys. Lett. **62**, 2119 (1993).

[12] L.B. Kiss, T. Larsson, P. Svedlindh, L. Lundgren, H. Ohlsen, M. Ottosson, J. Hudner, and L. Stolt, Physica C **207**, 318 (1993).

[13] A.M. Kadin, W.J.S. Skocpol, and M. Tinkham, J. Low Temp. Phys. **33**, 481 (1978).

[14] A.D. Semenov, R.S. Nebosis, Yu.P. Gousev, M.A. Heusinger, and K.F. Renk, Phys. Rev. B **52**, 581 (1995).

[15] Yu.P. Gousev, A.D. Semenov, A.V. Varlashkin, E.V. Pechen, R.S. Nebosis, and K.F. Renk, to be published in J. Appl. Phys. (1996).

[16] H.-W. Hübers, T.W. Crowe, G. Lundershausen, W.C.B. Peatman, and H.P. Röser, Proc. of the 4th Int. Symp. on Space Terahertz Tech., Los Angeles, CA, USA, March (1993).